JACS
JOURNAL OF THE AMERICAN CHEMICAL SOCIETY

Communication

Oxidative carbon backbone rearrangement in rishirilide biosynthesis

Olga Tsypik, Roman Makitrynskyy, Britta Frensch, David L. Zechel, Thomas Paululat, Robin Teufel, and Andreas Bechthold

J. Am. Chem. Soc., **Just Accepted Manuscript** • DOI: 10.1021/jacs.9b12736 • Publication Date (Web): 17 Mar 2020

Just Accepted

is published by the American Chemical Society. 1155 Sixteenth Street N.W., Washington, DC 20036

Oxidative carbon backbone rearrangement in rishirilide biosynthesis

Olga Tsypik[†], Roman Makitrynskyy[†], Britta Frensch[‡], David L. Zechel[§], Thomas Paululat[⁑], Robin Teufel[‡,*], and Andreas Bechthold[†,*]

[†] Department of Pharmaceutical Biology and Biotechnology, Institute of Pharmaceutical Sciences, Albert-Ludwigs-Universität Freiburg, Stefan-Meier-Strasse 19, 79104, Freiburg, Germany.

[‡] Faculty of Biology, Schänzlestr. 1, 79104, Freiburg, Germany.

[§] Department of Chemistry, Queen's University, 90 Bader Lane, Kingston, K7L 3N6 Ontario, Canada.

[⁑] Organic Chemistry, University of Siegen, Adolf-Reichwein-Str. 2, 57068 Siegen, Germany.

Supporting Information Placeholder

ABSTRACT: The structural diversity of type II polyketides is largely generated by tailoring enzymes. In rishirilide biosynthesis by *Streptomyces bottropensis*, ^{13}C-labelling studies previously implied extraordinary carbon backbone and sidechain rearrangements. In this work, we employ gene deletion experiments and *in vitro* enzyme studies to identify key biosynthetic intermediates and expose intricate redox tailoring steps for the formation of rishirilides A, B, D and lupinacidin A. First, the flavin-dependent RslO5 reductively ring opens the epoxide-moiety of an advanced polycyclic intermediate to form an alcohol. Then, flavin monooxygenase RslO9 oxidatively rearranges the carbon backbone, presumably via lactone-forming Baeyer-Villiger oxidation and subsequent intramolecular aldol condensation. While RslO9 can further convert the rearranged intermediate to rishirilide D and lupinacidin A, an additional ketoreductase RslO8 is required for formation of the main products rishirilide A and rishirilide B. This work provides insight into the structural diversification of aromatic polyketide natural products via unusual redox tailoring reactions that appear to defy biosynthetic logic.

Streptomycetes generate structurally diverse natural products with a wide spectrum of bioactivities, such as the type II polyketides[1] rishirilides A (**1**), B (**2**) and D (**3**) from *S. bottropensis*. These compounds act as inhibitors of α2-macroglobulin (**1** and **2**)[2] and *S*-glutathione reductase (**2**)[3] (**Scheme 1**). While four total syntheses of **2** have been reported,[4–7] little is known about rishirilide biosynthesis. Previous ^{13}C-labelling and NMR spectroscopic studies revealed that **2** is derived from an isobutyrate starter unit (generated from valine and malonyl-CoA) and eight malonyl-CoA extender units, the last of which undergoes an additional decarboxylation (Scheme 1).[8] The ^{13}C-labelling pattern furthermore implied an unusual oxidative rearrangement of the carbon backbone[2] (**Scheme 1**). In this study, the redox tailoring enzymes RslO5, RslO8, and RslO9, encoded by the rishirilide (*rsl*) biosynthetic gene cluster,[9] are shown to facilitate the key tailoring steps in rishirilide biosynthesis.

Initially, the roles of the predicted flavin-dependent enzymes RslO5 and RslO9 were examined, as flavoenzymes are mechanistically versatile[10–15] and often impart structural complexity to polyketide natural products.[11,13,16–18] The individual genes in *S. bottropensis* were replaced via double cross-overs with spectinomycin (*rslO5* mutant) or apramycin resistance genes (*rslO9* mutant) and the resulting mutants assayed for production of rishirilides by high resolution liquid chromatography mass spectrometry (HR-LCMS).

Relative to *S. bottropensis* (**Fig. 1A**), the Δ*rslO5* strain was deficient in the production of **1**, **2**, and **3**, but accumulated putative biosynthetic intermediates or shunt products (e.g., **4**) not observed in the native strain (**Fig. 1B**). To identify the substrate of RslO5, the enzyme was heterologously produced with an *N*-terminal His_6 tag and isolated with bound flavin mononucleotide (FMN) from *Escherichia coli* BL21 (DE3) Star™ (**Figs. S1A and S2**). Addition of RslO5 to a crude extract from the *S. bottropensis* Δ*rslO5* mutant in the presence of additional FMN and NAD(P)H led to the conversion of **4** (*m/z* = 367.117, $[M-H]^-$) into **5** (*m/z* = 369.133, $[M-H]^-$) (**Fig. 1C, S3 and S4**). Moreover, when RslO5 was incubated with purified **4** as a substrate, a clean reduction to **5** was observed in the presence of NADPH or NADH (**Figs. 2A and B**, **S5, S6, & S7**). In contrast, **4** was neither converted in assays with boiled RslO5, nor in assays containing only FMN and NADPH (**Fig. S7**). Next, **4** and **5** were purified from the respective mutants and analyzed by NMR spectroscopy (see **Supporting Information**). **4** proved to be an advanced intermediate with fully cyclized but non-rearranged carbon backbone and a surprising C3-C16 epoxide functionality. By contrast, **5** contained a C16-hydroxyl group most likely arising from the reductive epoxide ring opening of **4** (**Scheme 1**).

RslO5 is homologous to reductases of the Old Yellow Enzyme (OYE) family[19]. These enzymes typically catalyze two electron reductions of double bonds via hydride transfer, including those of α-β-unsaturated carbonyls and nitro-olefins. An amino acid sequence alignment of RslO5 with members of the OYE family (**Fig. S8**) revealed the conservation of Y177, H172, and N175. The corresponding amino acid residues H191 and N194 in OYE stabilize the transient enolate anion arising from initial hydride transfer, followed by Y196-dependent protonation to afford the reduced product.[19–21] For the conversion of **4** into **5**, we thus envisage a mechanism analogous to OYE for RslO5 (**Scheme 1**), possibly via a transient C17 oxyanion intermediate stabilized by H172 and N175. To further examine RslO5, enzyme variants were generated by site-directed mutagenesis. Unlike wild type RslO5, solutions of purified RslO5-H172N were clear, indicating a deficiency in FMN binding. Moreover, the RslO5-H172N variant was inactive when incubated with an extract containing **4** in the presence of FMN and NADPH (**Fig. 2C**). In contrast, the N175H and Y177F enzyme variants maintained the ability to bind FMN but showed significantly reduced activity (30 % and 11 % relative to wild type RslO5, respectively) (**Figs. 2D and E**, **S5** and **S6**), consistent with the proposed catalytic roles of the side chain residues.

Scheme 1. Proposed biosynthesis of rishirilides and side products by *S. bottropensis*. Compounds in boxes were characterized by NMR spectroscopy. The oxygen atom derived from O_2 is colored in red. Black and grey arrows indicate main enzyme reactions and (enzymatic

and non-enzymatic) side reactions, respectively. The pathway likely involves reduced hydroquinonic intermediates, which promote subsequent redox transformations (such as the epoxidation to **4**)[22–25].

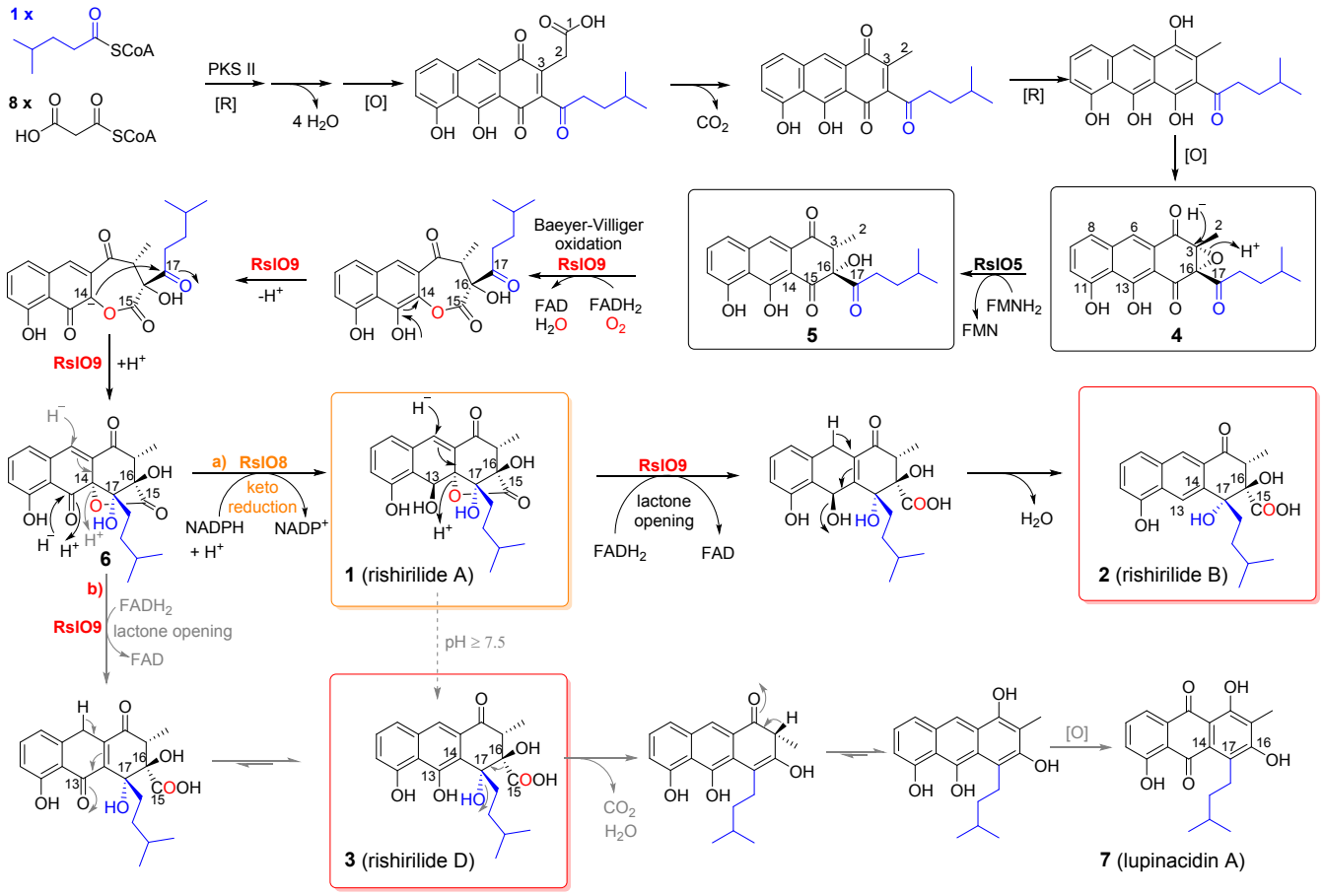

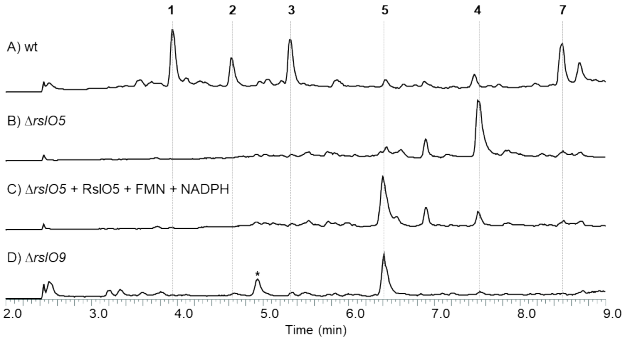

Figure 1. Gene inactivation studies of *rslO5* and *rslO9*. (A) TIC analysis of a culture extract from *S. bottropensis*. (B) Extract from *S. bottropensis* Δ*rslO5*. (C) Reaction of RslO5 with a crude extract from the Δ*rslO5* mutant with FMN and NADPH. (D) Extract from *S. bottropensis* Δ*rslO9*. The compound marked with asterisks (*) is a degradation product of **5** (structure not elucidated). The peak numbering corresponds to compounds in Scheme 1.

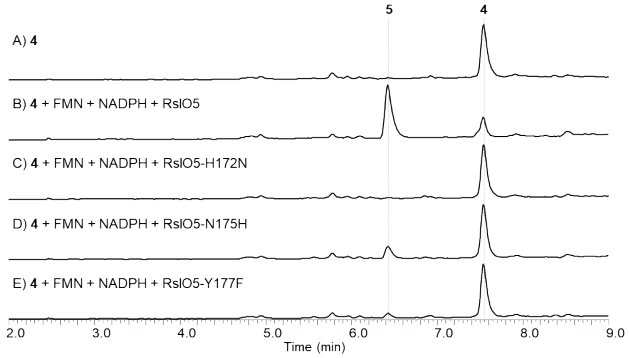

Figure 2. LC-MS (TIC) analysis of the conversion of **4** by RslO5 and active site variants. (A) Purified **4**; (B) **4** + RslO5 + FMN + NADPH; (C) **4** + RslO5-H172N + FMN + NADPH; (D) **4** + RslO5-N175H + FMN + NADPH; (E) **4** + RslO5-Y177F + FMN + NADPH. See **Figs. S5 and S6** for uncropped traces and EIC's.

As **5** also accumulated in the Δ*rslO9* mutant (but was prone to degradation) (**Fig. 1D**), it may represent RslO9's substrate. RslO9 is a prime candidate for catalyzing the central oxidative rearrangement steps in rishirilide biosynthesis because of homology to FAD-dependent Baeyer-Villiger monooxygenases such as MrqO6 (52% sequence identity / 95% sequence coverage), BexE (31% / 92%) and MtmOIV (36% / 46 %). Both MrqO6 and BexE perform key oxidative rearrangements during the biosynthesis of the angular aromatic polyketides murayaquinone and BE-7585A, respectively[26,27], while MtmOIV catalyzes

oxidative C–C bond cleavage in mithramycin biosynthesis.[28] RslO9 was heterologously produced with an *N*-terminal His_6 tag and contained a bound FAD cofactor after purification (**Figs. S1B** and **S2**). Indeed, RslO9 converted **5** to **3** (*m/z* = 387.144, $[M-H]^-$) in the presence of NADPH or NADH. In contrast, **5** was not converted in assays containing heat-denatured RslO9 or in assays lacking NAD(P)H (**Fig. 3** and **Figs. S9, S10, & S11**).

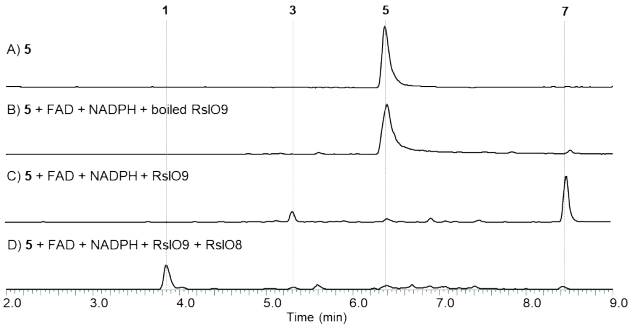

Figure 3. LC-MS (TIC) analysis of the reactions of RslO8 and RslO9 *in vitro*. (A) Chromatogram for purified **5**. (B) Incubation of **5** with heat inactivated RslO9. (C) Reaction of **5** with RslO9. (D) Reaction of **5** with RslO9 and RslO8. Reactions B, C, and D all included FAD and NADPH. See **Figs. S9 and S10** for uncropped traces and EIC's.

To further investigate the anticipated oxygenase functionality of RslO9, we conducted isotope-labelling experiments with $^{18}O_2$ (**Fig. S12**). Indeed, when **5** was converted by RslO9 in presence of $^{18}O_2$, the incorporation of one ^{18}O-atom into **3** was observed by HR-LCMS. Hence, we propose that RslO9 first inserts an oxygen atom between C14 and C15 via Baeyer-Villiger oxidation, before a C14-carbanion attacks the C17-ketone of the side chain to produce the postulated intermediate **6** (**Scheme 1**). Consistent with this mechanism, no incorporation of ^{18}O was observed when **5** was converted to **3** in the presence of $H_2{}^{18}O$ (**Fig. S12**). RslO9 may then further transform **6** into **3** via reduction of the central ring under concomitant lactone opening and following tautomerization (**Scheme 1**).

In order to corroborate the proposed pathway, we examined the RslO9-catalyzed reaction in more detail via discontinuous enzyme assays. In fact, the transient formation of an unstable compound with the expected mass of **6** (*m/z* = 385.129 $[M-H]^-$) was observed during the conversion of **5** into **3** (**Fig. 4**, **S13 and S14**). Moreover, following the isolation of **6** and subsequent incubation with RslO9 in *in vitro* assays, **3** was formed by RslO9 in addition to degradation products such as the predominant **7**, thus unambiguously identifying **6** as an intermediate in rishirilide biosynthesis (**Scheme 1**, **Figs. S15 and S16**). Although substrate reduction by a flavin monooxygenase as suggested for RslO9 appears perplexing, it has been reported for flavin monooxygenase ActVA involved in the biosynthesis of the type II polyketide actinorhodin[29]. It is noteworthy that **3** proved unstable and decomposed spontaneously to **7** (*m/z* = 339.123, $[M-H]^-$) and other minor compounds (**Figs. 1, 3 & 4** and **Fig. S17**). Based on MS and UV-Vis data[30], **7** is most likely the anti-tumorigenic lupinacidin A[31] that was recently reported to be produced by the rishirilide gene cluster[32]. **7** formation can be envisaged by decarboxylation of C15 of **3** and concurrent water elimination at C17, followed by tautomerization and autooxidation, as supported by ^{18}O-isotope labelling experiments (**Scheme 1**, **Fig. S12**).

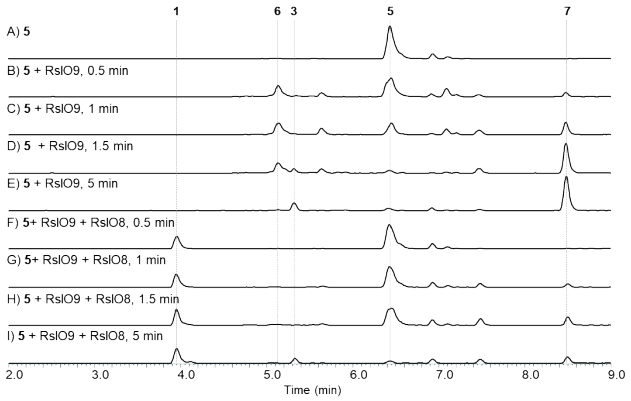

Figure 4. LC-MS (TIC) analysis of **6** formation during time-course reactions of RslO9 ± RslO8. (A) Chromatogram for purified **5**. (B) Incubation of **5** with RslO9 for 0.5 min, (C) 1 min, (D) 1.5 min and (E) 5 min. (F) Reaction of **5** with RslO9 and RslO8 incubated for 0.5 min, (G) 1 min, (H) 1.5 min and (I) 5 min. See **Figs. S13 and S14** for uncropped traces and EIC's. All reactions included NADPH.

The proposed structure of **6** implies that reduction of the C13-ketone to the respective hydroxyl group could afford **1**. We hypothesized that this step could be catalyzed by RslO8, which is 50% identical to the proposed enoyl-reductase ActVI-ORF2 from actinorhodin biosynthesis[33] and resembles medium chain dehydrogenases/reductases. These enzymes are typically composed of two domains: an *N*-terminal catalytic domain with homology to the folding chaperones GroEL and GroES; and a C-terminal Rossmann fold that binds NAD(P)H. To gain more insights into the function of RslO8, the *S. bottropensis* Δ*rslO8* mutant was generated. Compared to the wild type, inactivation of *rslO8* eliminated production of **1** and **2** in *S. bottropensis*, but increased the formation of **3** (**Figs. S18 and S19**), thus supporting a role for RslO8 in late stage rishirilide tailoring.

To further investigate this, *N*-terminal His_6 tagged RslO8 was produced and isolated from *E. coli* (**Fig. S1C**). As anticipated, *in vitro* assays of RslO8 and RslO9 with **5** as substrate afforded **1** and only minor amounts of **3** (**Fig. 3D**), whereas RslO8 alone did not convert **5**. RslO8 thus likely regio- and stereoselectively reduces the C13-ketone of **6** and thereby redirects the pathway toward **1** production. Consistent with this proposal, **3** was not accepted as a substrate by RslO8 in *in vitro* assays (**Fig. S17**). Crucially, isolated **6** could be reduced to **1** by RslO8 in presence of either NADH or NADPH, thus corroborating our biosynthetic proposal (**Figs. S15 and S16**). The structure of **1** suggests a possible lactone opening and conversion to **3** at higher pH values triggered by the deprotonation of C13. In fact, incubation of **1** at pH values ≥ 7.5 resulted in the spontaneous formation of **3** (**Scheme 1**, **Fig. S20**). **3** may thus represent both a shunt product arising from spontaneous degradation of **1** as well as an enzymatic side product from the competing activity of RslO9 and RslO8 for **6**. Finally, the generation of **2** from main product **1** could be rationalized by RslO9-mediated reduction of the central ring resulting in lactone opening, followed by water elimination (**Scheme 1**). Indeed, **1** was slowly converted to **2** in *in vitro* assays containing RslO9 and NADPH, in contrast to assays with boiled enzyme (**Figs. S21 and S22**). Taken together, **1** and **2** likely represent the main pathway products; yet the instability of **1** at higher pH values also promotes formation of the side products **3** and **7**.

In summary, this study establishes the key enzymatic tailoring reactions steps in rishirilide biosynthesis (for an overview of the gene cluster and the predicted functions of other encoded proteins,

see **Fig. S23**). The interplay between epoxide reductase RslO5, flavin monooxygenase RslO9, and ketoreductase RslO8 enables the intricate oxidative rearrangement of the polyketide carbon backbone and ultimately gives rise to structurally distinct rishirilides and lupinacidin A.

ASSOCIATED CONTENT

Supporting Information

The Supporting Information is available on the ACS Publications website at DOI:

Experimental procedures and compounds characterization data.

AUTHOR INFORMATION

Corresponding Authors

Prof. Dr. Andreas Bechthold, Department of Pharmaceutical Biology and Biotechnology, Institute of Pharmaceutical Sciences, Albert-Ludwigs-Universität Freiburg, Stefan-Meier-Strasse 19, 79104, Freiburg, Germany. E-mail: andreas.bechthold@pharmazie.uni-freiburg.de

Dr. Robin Teufel, Faculty of Biology, Schänzlestr. 1, 79104, Freiburg, Germany. E-mail: robin.teufel@zbsa.uni-freiburg.de.

Notes

The authors declare no competing financial interests.

ACKNOWLEDGMENTS

We thank Prof. Dr. J. Rohr, University of Kentucky, for fruitful discussion of our results and Dr. M. Myronovskyi, University of Saarbrucken, for kind assistance in HRMS analysis. The project was funded by the Deutsche Forschungsgemeinschaft (DFG, German Research Foundation) 235777276/GRK1976 (awarded to AB) and TE 931/2-1 (awarded to R.T.).

References

(1) Hertweck, C.; Luzhetskyy, A.; Rebets, Y.; Bechthold, A. Type II polyketide synthases: gaining a deeper insight into enzymatic teamwork. *Nat. Prod. Rep.* **2007**, *24*, 162–190.

(2) Iwaki, H.; Nakayama, Y.; Takahashi, M.; Uetsuki, S.; Kido, M.; Fukuyama, Y. Structures of rishirilides A and B, alpha 2-macroglobulin inhibitors produced by *Streptomyces rishiriensis* OFR-1056. *J. Antibiot.* **1984**, *37*, 1091–1093.

(3) Komagata, D.; Sawa, R.; Kinoshita, N.; Imada, C.; Sawa, T.; Naganawa, H.; Hamada, M.; Okami, Y.; Takeuchi, T. Isolation of glutathione-S-transferase inhibitors. *J. Antibiot.* **1992**, *45*, 1681–1683.

(4) Allen, J. G.; Danishefsky, S. J. The total synthesis of (+/-)-rishirilide B. *J. Am. Chem. Soc.* **2001**, *123*, 351–352.

(5) Yamamoto, K.; Hentemann, M. F.; Allen, J. G.; Danishefsky, S. J. On the total synthesis and determination of the absolute configuration of rishirilide B: exploitation of subtle effects to control the sense of cycloaddition of o-quinodimethides. *Chemistry* **2003**, *9*, 3242–3252.

(6) Mejorado, L. H.; Pettus, T. R. R. Total synthesis of (+)-rishirilide B: development and application of general processes for enantioselective oxidative dearomatization of resorcinol derivatives. *J. Am. Chem. Soc.* **2006**, *128*, 15625–15631.

(7) Odagi, M.; Furukori, K.; Takayama, K.; Noguchi, K.; Nagasawa, K. Total Synthesis of Rishirilide B by Organocatalytic Oxidative Kinetic Resolution: Revision of Absolute Configuration of (+)-Rishirilide B. *Angew. Chem. Int. Ed. Engl.* **2017**, *56*, 6609–6612.

(8) Schwarzer, P.; Wunsch-Palasis, J.; Bechthold, A.; Paululat, T. Biosynthesis of Rishirilide B. *Antibiotics (Basel)* **2018**, *7*.

(9) Yan, X.; Probst, K.; Linnenbrink, A.; Arnold, M.; Paululat, T.; Zeeck, A.; Bechthold, A. Cloning and heterologous expression of three type II PKS gene clusters from Streptomyces bottropensis. *Chembiochem* **2012**, *13*, 224–230.

(10) Matthews, A.; Saleem-Batcha, R.; Sanders, J. N.; Stull, F.; Houk, K. N.; Teufel, R. Aminoperoxide adducts expand the catalytic repertoire of flavin monooxygenases. *Nat. Chem. Biol.* [Online early access]. DOI: 10.1038/s41589-020-0476-2.

(11) Walsh, C. T.; Wencewicz, T. A. Flavoenzymes: versatile catalysts in biosynthetic pathways. *Nat. Prod. Rep.* **2013**, *30*, 175–200.

(12) Teufel, R.; Miyanaga, A.; Michaudel, Q.; Stull, F.; Louie, G.; Noel, J. P.; Baran, P. S.; Palfey, B.; Moore, B. S. Flavin-mediated dual oxidation controls an enzymatic Favorskii-type rearrangement. *Nature* **2013**, *503*, 552–556.

(13) Teufel, R.; Agarwal, V.; Moore, B. S. Unusual flavoenzyme catalysis in marine bacteria. *Curr. Op. Chem. Biol.* **2016**, *31*, 31–39.

(14) Fraaije, M. W.; Mattevi, A. Flavoenzymes: diverse catalysts with recurrent features. *Trends Biochem. Sci.* **2000**, *25*, 126–132.

(15) Huijbers, M. M. E.; Montersino, S.; Westphal, A. H.; Tischler, D.; van Berkel, W. J. H. Flavin dependent monooxygenases. *Arch. Biochem. Biophys.* **2014**, *544*, 2–17.

(16) Teufel, R.; Stull, F.; Meehan, M. J.; Michaudel, Q.; Dorrestein, P. C.; Palfey, B.; Moore, B. S. Biochemical Establishment and Characterization of EncM's Flavin-N5-oxide Cofactor. *J. Am. Chem. Soc.* **2015**, *137*, 8078–8085.

(17) Yunt, Z.; Reinhardt, K.; Li, A.; Engeser, M.; Dahse, H.-M.; Gütschow, M.; Bruhn, T.; Bringmann, G.; Piel, J. Cleavage of four carbon-carbon bonds during biosynthesis of the griseorhodin a spiroketal pharmacophore. *J. Am. Chem. Soc.* **2009**, *131*, 2297–2305.

(18) Teufel, R. Flavin-catalyzed redox tailoring reactions in natural product biosynthesis. *Arch. Biochem. Biophys.* **2017**, *632*, 20–27.

(19) Meah, Y.; Brown, B. J.; Chakraborty, S.; Massey, V. Old yellow enzyme: reduction of nitrate esters, glycerin trinitrate, and propylene 1,2-dinitrate. *Proc. Natl. Acad. Sci. U.S.A.* **2001**, *98*, 8560–8565.

(20) Meah, Y.; Massey, V. Old yellow enzyme: stepwise reduction of nitro-olefins and catalysis of aci-nitro tautomerization. *Proc. Natl. Acad. Sci. U.S.A.* **2000**, *97*, 10733–10738.

(21) Brown, B. J.; Deng, Z.; Karplus, P. A.; Massey, V. On the active site of Old Yellow Enzyme. Role of histidine 191 and asparagine 194. *J. Biol. Chem.* **1998**, *273*, 32753–32762.

(22) Conradt, D.; Schätzle, M. A.; Haas, J.; Townsend, C. A.; Müller, M. New Insights into the Conversion of Versicolorin A in the Biosynthesis of Aflatoxin B1. *J. Am. Chem. Soc.* **2015**, *137*, 10867–10869.

(23) Husain, S. M.; Schätzle, M. A.; Lüdeke, S.; Müller, M. Unprecedented role of hydronaphthoquinone tautomers in biosynthesis. *Angew. Chem.* **2014**, *53*, 9806–9811.

(24) Schätzle, M. A.; Husain, S. M.; Ferlaino, S.; Müller, M. Tautomers of anthrahydroquinones: enzymatic reduction and implications for

chrysophanol, monodictyphenone, and related xanthone biosyntheses. *J. Am. Chem. Soc.* **2012**, *134*, 14742–14745.

(25) Hashimoto, M.; Taguchi, T.; Ishikawa, K.; Mori, R.; Hotta, A.; Watari, S.; Katakawa, K.; Kumamoto, T.; Okamoto, S.; Ichinose, K. Unveiling Two Consecutive Hydroxylations: Mechanisms of Aromatic Hydroxylations Catalyzed by Flavin-Dependent Monooxygenases for the Biosynthesis of Actinorhodin and Related Antibiotics. *Chembiochem* [Online early access]. DOI: 10.1002/cbic.201900490.

(26) Gao, G.; Liu, X.; Xu, M.; Wang, Y.; Zhang, F.; Xu, L.; Lv, J.; Long, Q.; Kang, Q.; Ou, H.-Y.; Wang, Y.; Rohr, J.; Deng, Z.; Jiang, M.; Lin, S.; Tao, M. Formation of an Angular Aromatic Polyketide from a Linear Anthrene Precursor via Oxidative Rearrangement. *Cell Chem. Biol.* **2017**, *24*, 881-891.e4.

(27) Jackson, D.R.; Yu, X.; Wang, G.; Patel, A.B.1; Calveras, J.; Barajas, J.F.; Sasaki, E.; Metsä-Ketelä, M.; Liu, H.W.3; Rohr, J.; Tsai, S.C. Insights into Complex Oxidation during BE-7585A Biosynthesis: Structural Determination and Analysis of the Polyketide Monooxygenase BexE. *ACS Chem. Biol*. **2016,** *11*, 1137-1147.

(28) Bosserman, M. A.; Downey, T.; Noinaj, N.; Buchanan, S. K.; Rohr, J. Molecular insight into substrate recognition and catalysis of Baeyer-Villiger monooxygenase MtmOIV, the key frame-modifying enzyme in the biosynthesis of anticancer agent mithramycin. *ACS Chem. Biol.* **2013**, *8*, 2466–2477.

(29) Valton, J.; Mathevon, C.; Fontecave, M.; Nivière, V.; Ballou, D. P. Mechanism and regulation of the Two-component FMN-dependent monooxygenase ActVA-ActVB from Streptomyces coelicolor. *J. Biol. Chem.* **2008**, *283*, 10287–10296.

(30) Sottorff, I.; Künzel, S.; Wiese, J.; Lipfert, M.; Preußke, N.; Sönnichsen, F. D.; Imhoff, J. F. Antitumor Anthraquinones from an Easter Island Sea Anemone: Animal or Bacterial Origin? *Mar. Drugs* **2019**, *17*.

(31) Igarashi, Y.; Trujillo, M. E.; Martínez-Molina, E.; Yanase, S.; Miyanaga, S.; Obata, T.; Sakurai, H.; Saiki, I.; Fujita, T.; Furumai, T. Antitumor anthraquinones from an endophytic actinomycete Micromonospora lupini sp. nov. *Bioorg. Med. Chem. Lett.* **2007**, *17*, 3702–3705.

(32) Zhang, C.; Sun, C.; Huang, H.; Gui, C.; Wang, L.; Li, Q.; Ju, J. Biosynthetic Baeyer-Villiger Chemistry Enables Access to Two Anthracene Scaffolds from a Single Gene Cluster in Deep-Sea-Derived *Streptomyces olivaceus* SCSIO T05. *J. Nat. Prod.* **2018**, *81*, 1570–1577.

(33) Taguchi, T.; Itou, K.; Ebizuka, Y.; Malpartida, F.; Hopwood, D. A.; Surti, C. M.; Booker-Milburn, K. I.; Stephenson, G. R.; Ichinose, K. Chemical characterisation of disruptants of the Streptomyces coelicolor A3(2) actVI genes involved in actinorhodin biosynthesis. *J. Antibiot.* **2000**, *53*, 144–152.

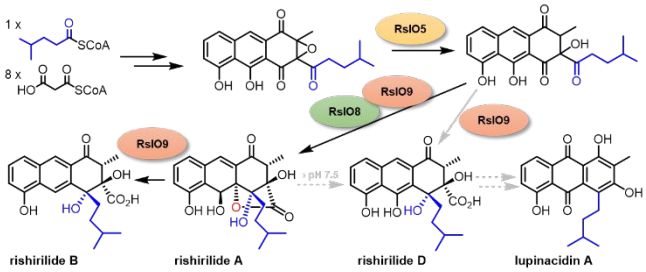

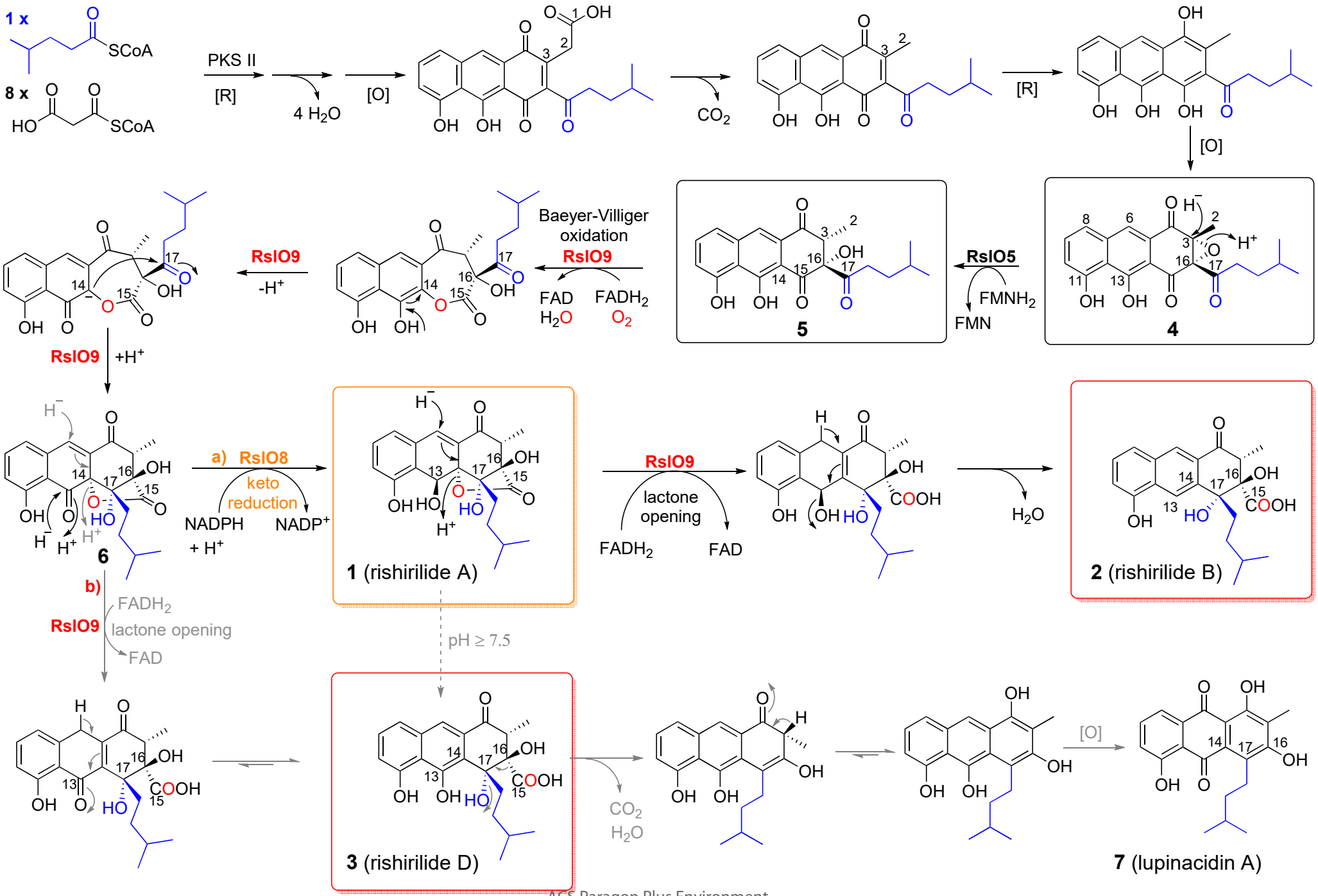
1 x
8 x
SCoA
HO
PKS II
[R]
4 H2O
[O]
CO2
[R]
[O]
RslO5
FMNH2
FMN
4
5
Baeyer-Villiger oxidation
RslO9
FAD
H2O
FADH2
O2
RslO9
-H+
RslO9
+H+
6
a) RslO8
keto reduction
NADPH
+ H+
NADP+
1 (rishirilide A)
RslO9
lactone opening
FADH2
FAD
H2O
2 (rishirilide B)
b)
RslO9
FADH2
lactone opening
FAD
pH ≥ 7.5
3 (rishirilide D)
CO2
H2O
[O]
7 (lupinacidin A)

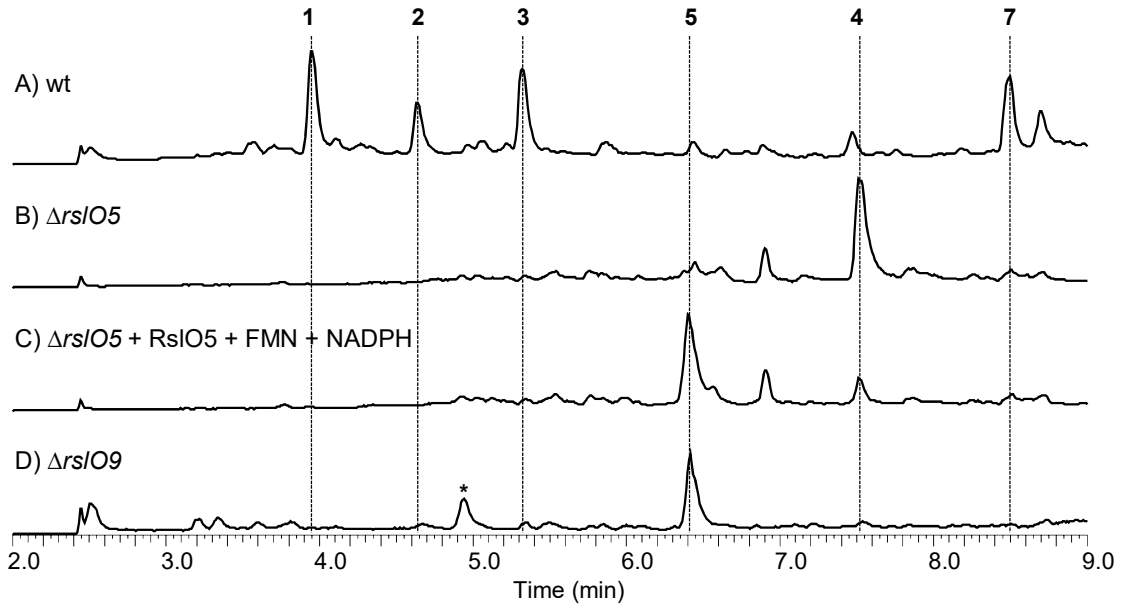
1
2
3
5
4
7
A) wt
B) ΔrslO5
C) ΔrslO5 + RslO5 + FMN + NADPH
D) ΔrslO9
*
2.0
3.0
4.0
5.0
6.0
7.0
8.0
9.0
Time (min)

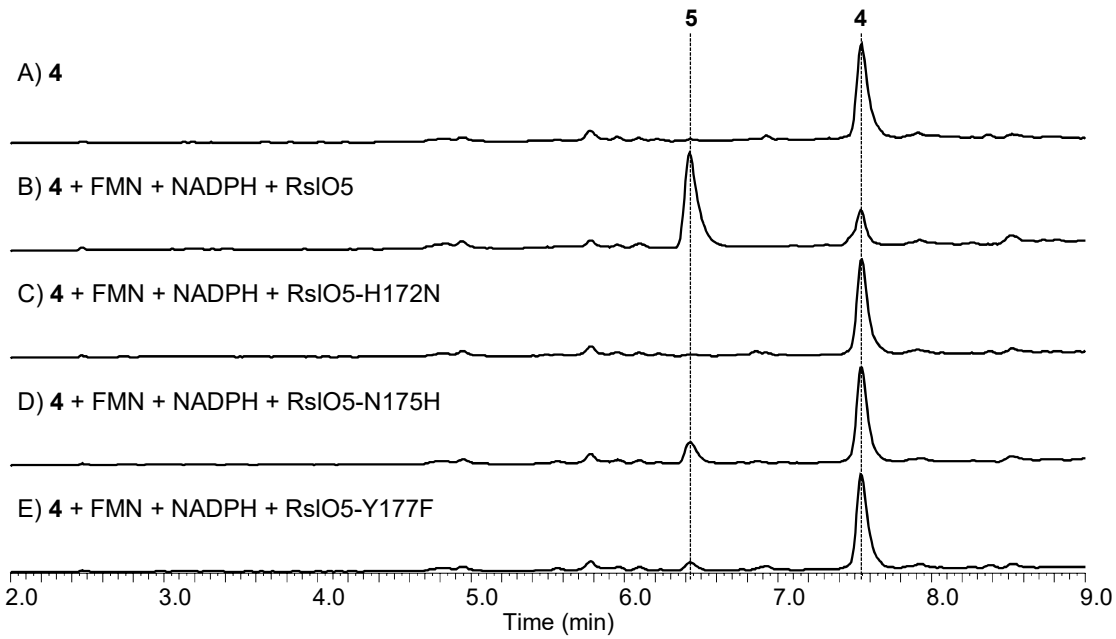
5
4
A) 4
B) 4 + FMN + NADPH + RslO5
C) 4 + FMN + NADPH + RslO5-H172N
D) 4 + FMN + NADPH + RslO5-N175H
E) 4 + FMN + NADPH + RslO5-Y177F
2.0
3.0
4.0
5.0
6.0
7.0
8.0
9.0
Time (min)

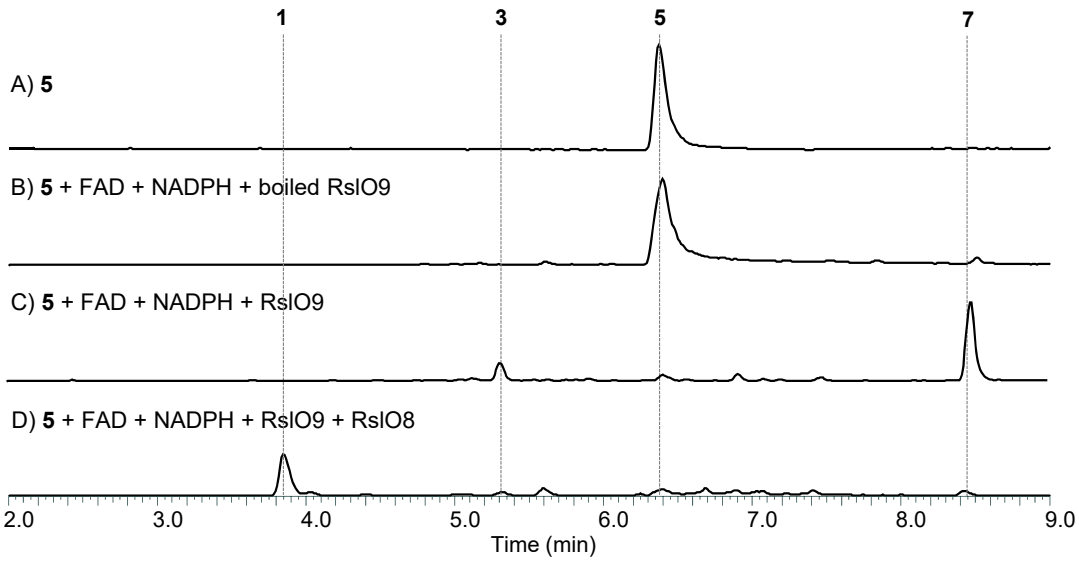
1
3
5
7
A) 5
B) 5 + FAD + NADPH + boiled RslO9
C) 5 + FAD + NADPH + RslO9
D) 5 + FAD + NADPH + RslO9 + RslO8
2.0
3.0
4.0
5.0
6.0
7.0
8.0
9.0
Time (min)

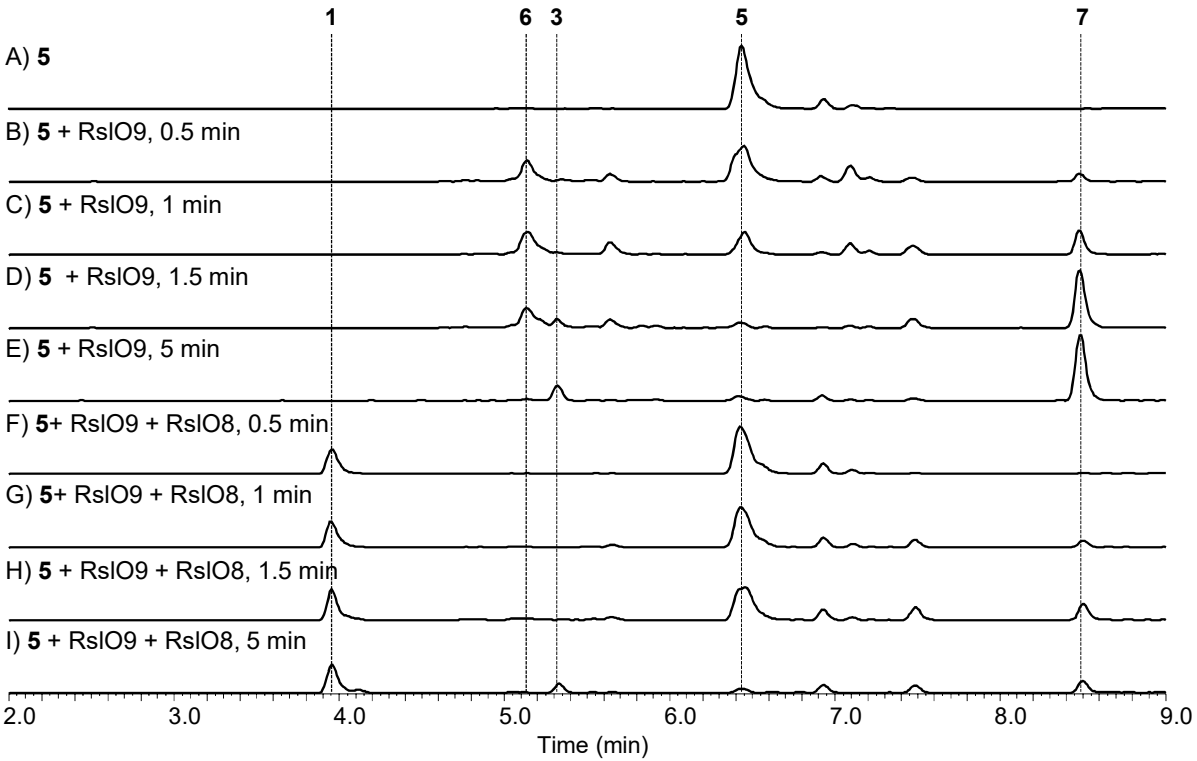
1
6
3
5
7
A) 5
B) 5 + RslO9, 0.5 min
C) 5 + RslO9, 1 min
D) 5 + RslO9, 1.5 min
E) 5 + RslO9, 5 min
F) 5+ RslO9 + RslO8, 0.5 min
G) 5+ RslO9 + RslO8, 1 min
H) 5 + RslO9 + RslO8, 1.5 min
I) 5 + RslO9 + RslO8, 5 min
2.0
3.0
4.0
5.0
6.0
7.0
8.0
9.0
Time (min)